MODELING OF SEA STATE CONDITIONS FOR IMPROVEMENT OF CYGNSS L2 WIND SPEED RETRIEVALS

Tianlin Wang[1], Valery U. Zavorotny[2], Joel Johnson[3], Christopher Ruf[1], Yuchan Yi[4]

[1]University of Michigan, Ann Arbor, MI USA
[2]NOAA Earth System Research Laboratory, Physical Sciences Division, Boulder, CO USA
[3]ElectroScience Laboratory, The Ohio State University, Columbus, OH USA
[4]School of Earth Sciences, The Ohio State University, Columbus, OH USA

ABSTRACT

The Level 2 data product of the Cyclone Global Navigation Satellite System (CYGNSS) mission includes the retrieved ocean surface wind speed and the mean square slope (MSS), which are derived from the Level 1 normalized bistatic radar cross section (NBRCS). In the current L2 retrieval algorithm, the wind speed is retrieved using empirical geophysical model functions (GMFs) based on matchups with ground truth wind speed. However, sea state conditions, including the presence of external swell and the degree of wave development, complicate the ocean surface wave spectra and increase the uncertainty of the wind speed retrieval. An excess MSS approach is proposed to model sea state conditions. It calculates the excess MSS responsible for the sea state condition effects using ancillary data and the Elfouhaily *et al.* wave spectral model. A case study demonstrates that this approach reduces the wave effect (due to the sea state condition) on the CYGNSS NBRCS and improves the L2 wind speed retrieval.

Index Terms**—** CYGNSS, wind speed, mean square slope (MSS), sea state

1. INTRODUCTION

The Cyclone Global Navigation Satellite System (CYGNSS) mission aims to measure the ocean surface wind speed, including wind speeds in tropical cyclones [1]. The Level 1 calibration algorithm converts the Delay Doppler Maps (DDMs) measured by CYGNSS into normalized bistatic radar cross section (NBRCS) [2]. The Level 2 retrieval algorithm uses the calibrated NBRCS to retrieve the wind speed and to compute the mean square slope (MSS).

The current baseline L2 algorithm for the wind speed was developed by 1) assembling DDM observables with ground truth wind speed and incidence angles; 2) generating empirical 2D GMFs, including fully developed seas and limited-fetch (young) seas; and 3) mapping from the DDM to estimated wind speed based on the developed GMFs [2].

The baseline retrieval algorithm divides the sea state into two different types – a "fully developed" type and a "limited fetch" type. The fully developed sea has a sea state independent of the wind forcing extent (fetch) and/or duration, while the limited fetch sea is typical for situations when the wind is not constant in speed and direction, such as in hurricanes. This division oversimplifies the large variety of sea state behaviors that may occur. It also does not account for the possible presence of swell generated by distant wind systems [2].

An attempt to tie the measured NBRCS (or MSS) to the wind speed alone shows significant residual errors (scatter), which have also been observed in TechDemoSat-1 (TDS-1) retrievals [3]. The error in wind speeds retrieved from the observations is strongly correlated with the significant wave height (SWH) of the ocean [4]. A similar scatter is observed in the first wind speed and MSS retrievals based on the CYGNSS data. These results show that there is a necessity to take into account the sea state influence on the MSS, especially the non-local swell contribution to the surface roughness. Also, understanding the L-band signal response to both waves and wind will be helpful to provide higher accuracy L2 data products for wind speed and MSS.

An excess MSS approach for the L2 wind speed retrieval algorithm is proposed. The excess MSS, responsible for sea-state development effects, is defined as the difference between the MSS calculated using the IFREMER (Institut Francais de Recherche pour l'Exploitation de la MER) implementation of the WaveWatch III (WW3) numerical model [5] and the MSS calculated using a version of the Elfouhaily *et al*. spectral model [6] for fully developed seas. Subtracting it from the CYGNSS measured MSS, the resulting MSS should then be dependent only on the local wind. This will lead to a more accurate GMF for wind speed retrievals. A more advanced approach would model both the local wind and non-local swell spectra for the purpose of a consistency check between the measured MSS, the MSS and SWH modeled with the WW3, and ancillary SWH data.

2. PHYSICAL BASIS

2.1. Ocean Wave Spectra, MSS and SWH

The specular NBRCS measured by CYGNSS has the form under the geometrical optics (GO) approximation (less applicable for wind speed < 5 m/s):

$$\sigma_0^{CY} = |R|^2/2\sigma_u\sigma_c \quad (1)$$

where R is the complex Fresnel coefficient for left-hand circular polarization (LHCP), $2\sigma_u\sigma_c$ is the surface MSS, 'u' and 'c' refer to upwind and crosswind, respectively. The baseline equation used for CYGNSS L2 MSS computation is

$$s_{CY}^2 = |R|^2/\sigma_0^{CY} \quad (2)$$

Physically, MSS can be modeled as a weighted integration over the sea surface spectrum,

$$s_{Model}^2 = 2\sigma_u\sigma_c = 2\left[\int_0^{\kappa_{cut}} d\vec{\kappa}\,\Psi(\vec{\kappa})\kappa^2\cos^2\varphi\right]^{\frac{1}{2}}\left[\int_0^{\kappa_{cut}} d\vec{\kappa}\,\Psi(\vec{\kappa})\kappa^2\sin^2\varphi\right]^{\frac{1}{2}} \quad (3)$$

where the cutoff frequency $\kappa_{cut} = k_0(\cos\theta_{SP})/3$, with k_0 the electromagnetic wavenumber and θ_{SP} the specular incidence angle.

To model the MSS, knowledge of the ocean surface wave spectrum $\Psi(\vec{\kappa})$ is required. If non-local swell is present that does not interact with the waves driven by the local wind, then the total spectrum can be computed by

$$\Psi(\vec{\kappa}) = \Psi_{local}(\vec{\kappa}) + \Psi_{swell}(\vec{\kappa}) \quad (4)$$

where $\Psi_{local}(\vec{\kappa})$ is the short wave spectrum driven by the local wind, and $\Psi_{swell}(\vec{\kappa})$ is the long wave spectrum driven by the non-local swell.

SWH uses a different integration over the wave spectra,

$$H_s = 4\langle\eta^2\rangle^{1/2} \quad (5)$$

where the variance of the surface $\langle\eta^2\rangle$ is

$$\langle\eta^2\rangle = \iint_0^{\kappa_{cut}} d^2\kappa\,[\Psi_{local}(\vec{\kappa}) + \Psi_{swell}(\vec{\kappa})] \quad (6)$$

Comparing (3) and (6), due to the κ^2 factor, we can conclude that: 1) the MSS is more sensitive to the contributions of shorter waves; 2) the SWH is more sensitive to the contributions of longer waves; 3) the SWH is dominated by the larger amplitude long waves.

2.2. Wave Spectra for Local Wind and Swell

The ideal case presented in (4) exists when there is a clear separation between the swell and the wind spectra. This happens when the non-local swell is long enough, whereas the local wind driven waves are all short waves and the wind speed is sufficiently low. However, when the wind speed increases, long wave components might emerge in the local wind spectra which makes the separation of two spectra more difficult.

Also as reported in the Wind and Salinity Experiment (WISE) 2001 field campaign [7, 8], in the high frequency (short wave) region, the measured spectrum matches the wind driven wave spectrum well. However, in the low frequency (long wave) region, they are strongly different. The disagreement is explained by taking into account the influence of a swell spectrum. It should be noted that: 1) the local wind driven spectrum is wider with a smaller amplitude and with a peak position in the high frequency region; 2) the swell spectrum is typically narrower, with a larger amplitude and with a peak position in the low frequency region. The WISE 2001 campaign measurements indicate that local wind and swell spectra may be easily mixed, and they need to be separated in the ancillary wave modeling.

The wave spectrum driven by the local wind has been intensively studied. Elfouhaily *et al.* developed an omnidirectional and wind-dependent spectrum as a wavenumber spectrum which has a unifying feature of wave age parameterization [6]. The Elfouhaily *et al.* spectrum is defined as

$$\Psi_{local}(\vec{\kappa}) = \kappa^{-4}B(\kappa)D(\kappa,\varphi) \quad (7)$$

where $D(\kappa,\varphi)$ is the directional part of the spectrum and $B(\kappa)$ is the curvature spectrum defined as

$$B(\kappa) = 3\times10^{-3}\sqrt{\frac{\Omega\kappa}{\kappa_p}}exp\left[-\frac{\Omega}{\sqrt{10}}\left(\sqrt{\frac{\kappa_p}{\kappa}} - 1 - \frac{4}{5}\left(\frac{\kappa_p}{\kappa}\right)^2\right)\right]\Gamma^{\Upsilon(\kappa)} \quad (8)$$

where Ω is the inverse wave age ($\Omega = 0.84$ for infinite fetch), and the wave number of the spectral peak κ_p is

$$\kappa_p = g(\Omega/U_{10})^2 \quad (9)$$

where U_{10} is wind speed and g is gravity acceleration.

The two key input parameters are: 1) the wind speed U_{10}, where Elfouhaily *et al.* model is only applicable to wind speed range 2 m/s to 24 m/s; 2) the inverse wave age Ω, which is defined as

$$\Omega = 0.84/\{\tanh[(X/X_0)^{0.4}]\}^{0.75} \quad (10)$$

where $X_0 = 2.2\times10^4$, $X = fetch\cdot k_0$, $k_0 = g/(U_{10})^2$. By using Ω, we can define the sea state as fully developed or limited fetch (young). Therefore, the sea state could have a significant impact on the MSS.

For the swell spectrum, a narrow-band Gaussian process was used to match the WISE 2001 campaign roughness measurement in [7]. A swell index model is developed by Hwang for the spectral parameterization to investigate the swell influence [9].

3. EXCESS MSS APPROACH

Figure 1 illustrates the physical insights basis for extracting the wind dependent portion of the CYGNSS MSS using WW3 numerical data. The IFREMER WW3 numerical model generates MSS based on the slope spectrum by integrating it up to the WW3 cutoff of 2.1 rad/m. The CYGNSS MSS has a cutoff frequency between 4 and 12 rad/m, depending on the specular incidence angle.

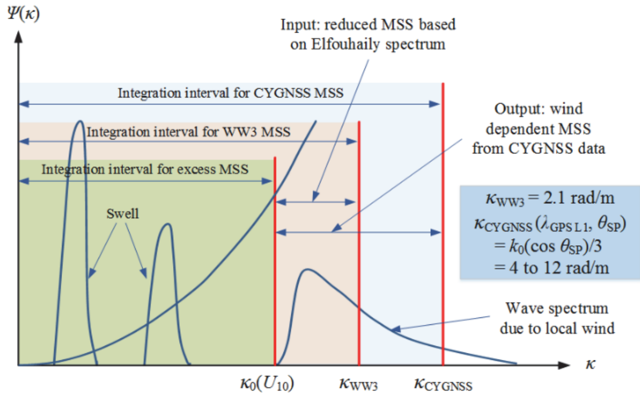

Figure. 1 Physics of extracting wind dependent MSS

An assumption is made that the excess MSS due to swells (at the lower end of spectrum) is separated from the wind dependent MSS (at the higher end of spectrum). Within this approach, modeling of sea state conditions means calculation of the excess MSS responsible for the sea state condition effects. After subtracting it from the CYGNSS MSS we create a modified MSS that is intended to correspond to the local wind much better than the initial MSS.

We assume that we have access to a wave model that takes input wind fields U_{10}, and produces the wave spectrum $\Psi_{WW}(\vec{\kappa})$, and based on it (using (3)), the WW3 MSS $\tilde{s}^2_{WW}(\vec{\kappa})$. It should be noted that the cutoff wavenumber κ_{cut} in this case is that of the WW3 model runs. Similarly, if the sea were assumed to be fully developed, we also have a one-to-one mapping between the wind speed U_{10} and MSS $\tilde{s}^2_{FD}(\vec{\kappa})$ under an assumed spectrum $\Psi_{FD}(\vec{\kappa})$.

Then, the excess MSS is computed as

$$\Delta\tilde{s}^2 = \tilde{s}^2_{WW}(\vec{\kappa}) - \tilde{s}^2_{FD}(\vec{\kappa}) \tag{11}$$

which is the WW3 model prediction of the influence of all sea state, e.g. wave age, limited fetch, non-local swell, etc.

The next step is to compute the wind dependent MSS by subtracting the excess MSS from the CYGNSS MSS

$$\tilde{s}^2_{CY} = s^2_{CY} - \Delta\tilde{s}^2 \tag{12}$$

A wind speed retrieval is then attempted by converting $\tilde{s}^2_{CY}$ back into a corrected NBRCS using (2) and performing a retrieval using the GMFs.

Ancillary matchup data used include the wind speed (ECMWF (European Centre for Medium-Range Weather Forecasts) and GDAS (Global Data Assimilation System) for low wind speed, SFMR (Stepped-Frequency Microwave Radiometer) for high wind speed), and MSS and SWH from WW3.

4. RESULTS AND ANALYSIS

A study case is considered from one segment of CYGNSS data on April 8th, 2017, using the observatory FM01, channel 4, with a signal from GPS PRN = 10, covering 31640-31850 seconds of the day. The track of the specular point was over the northeast Pacific Ocean. The matchup wind speed was relatively low, and the SWH was large.

Figure 2 shows the time-series MSS: raw CYGNSS L2 MSS, IFREMER MSS of WW3, and the reduced MSS based on the Elfouhaily *et al.* spectrum. The raw CYGNSS L2 MSS is higher than the IFREMER MSS due to the larger cutoff frequency. The reduced MSS is calculated using the matchup ECMWF wind speed and an inverse wave age $\Omega = 0.84$ for fully developed sea. It is much lower than both the measured and numerically modeled MSS, which indicates that there is a strong wave effect due to the sea state. The blank part of the reduced MSS time series is due to wind speeds below the lower wind speed limit of the Elfouhaily *et al.* spectrum, 2 m/s. Those points have been forced to be zero since the wind driven MSS should be very small at the low wind speed.

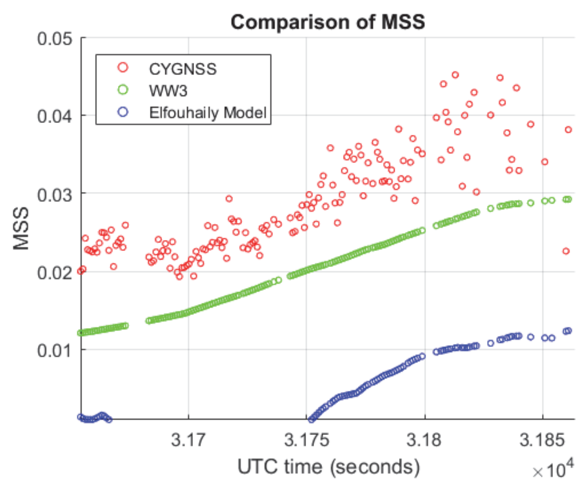

Figure. 2 Comparison of time-series MSS

Figure 3 shows a scatter plot of the excess MSS (WW3 MSS subtracted by the reduced MSS vs. SWH of WW3). It demonstrates a strong positive correlation between the excess MSS and the SWH. This confirms that the sea state (e.g. non-local swell) could have a significant impact on the MSS.

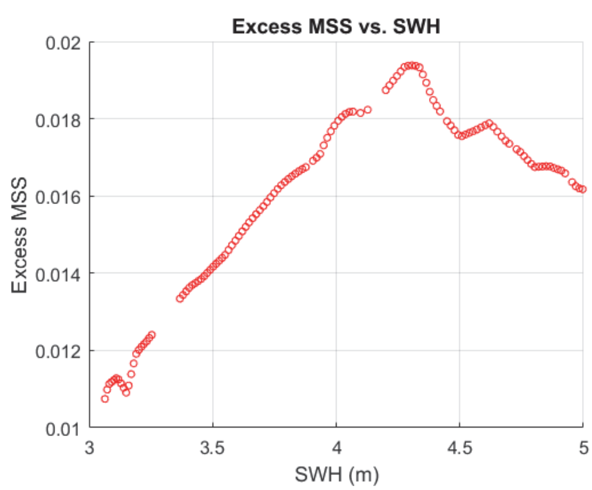

Figure. 3 Excess MSS vs. SWH of WW3

Figure 4 shows the time-series of retrieved wind speed using the raw and the corrected CYGNSS NBRCS as well as the matchup wind speeds from ECMWF and GDAS. The root mean square difference (RMSD) between the retrieved wind speed and ECMWF wind speed is reduced from 6.48 m/s to 1.15 m/s.

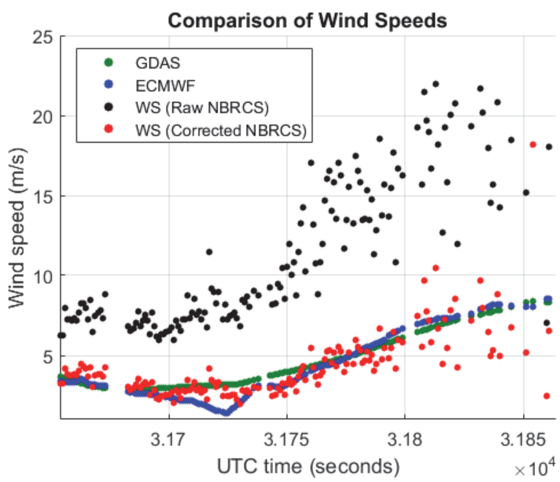

Figure. 4 Comparison of time-series wind speeds

This case study shows that the excess MSS approach effectively captures the wave effect (due to sea state conditions) on the CYGNSS observation. The approach significantly improves the L2 wind speed retrieval for the case of low wind speed and large SWH.

6. CONCLUSION AND FUTURE WORK

In this paper, we discuss sea surface modeling, its impact on the MSS surface roughness parameter, and how this can lead to the improvement of CYGNSS L2 wind speed retrievals. An excess MSS approach is proposed for modeling sea state conditions through computation of the excess MSS and modeling of the local wave and non-local swell spectra. A case study using real CYGNSS data demonstrates that the excess MSS approach can improve the accuracy of the CYGNSS L2 wind speed retrieval.

Future work includes the follows:

1). Apply this approach to a larger data set to better test the improvement of the wind speed retrieval and to study the statistical behavior of excess MSS in different seasons and at different geolocations, etc.

2). Generate a feedback signal and develop a closed-loop algorithm by running the WW3 model and iterating the calculation of the excess MSS for better accuracy of sea state modeling and wind speed retrieval.

3). Develop a modified forward model as an addition to the current model used in the CYGNSS End-to-End Simulator (E2ES), adding an MSS calculation based on the spectra driven by the local wind and the non-local swell rather than the current empirical Katzberg *et al.* model [10], as well as use of the first-order small slope approximation (SSA1) for the regime of weak diffusive scattering in the low wind speed case (wind speed < 5 m/s) [11].

4). For more in-depth modeling of sea state conditions, the modeling of both local wind and non-local swell spectra is proposed within the spectrum-based approach. Mainly, its purpose is to check for consistency between the measured MSS, the MSS and SWH modeled with the WW3, and with ancillary SWH data.

More testing of the effectiveness of these approaches for mitigating swell-induced effects on CYGNSS wind speed retrievals is currently in progress; results will be reported in the conference presentation.

7. REFERENCES

[1] C. S. Ruf, A. Lyons, M. Unwin, J. Dickinson, R. Rose, D. Rose, and M. Vincent, "CYGNSS: Enabling the Future of Hurricane Prediction," *IEEE Geosci. Remote Sens. Mag.*, vol. 1, no. 2, pp. 52-67, June 2013.

[2] Ruf, C. S., et al., *CYGNSS Handbook*, Michigan Publishing, Ann Arbor, MI, 2016.

[3] G. Foti, C. Gommenginger, P. Jales, M. Unwin, A. Shaw, C. Robertson, and J. Roselló, "Spaceborne GNSS Reflectometry for Ocean Winds: First Results from the UK TechDemoSat-1 Mission," *Geophys. Res. Lett.*, vol. 42, no. 13, pp. 5435-5441, July 2015.

[4] M. P. Clarizia, C. S. Ruf, "Bayesian Wind Speed Estimation Conditioned on Significant Wave Height for GNSS-R Ocean Observations," *J. Atmos. Ocean. Tech.*, vol. 34, no.6, pp.1193-1202, June 2017.

[5] WaveWatch III Development Group, "User Manual and System Documentation of WaveWatch III Version 5.16," MMAB Technical Note, Oct. 2016.

[6] T. Elfouhaily, B. Chapron, and K. Katsaros, "A Unified Directional Spectrum for Long and Short Wind-driven Waves," *J. Geophys. Res.*, vol. 102, no. C7, pp. 15781-15796, July 1997.

[7] Camps, A. et al., "Wind and Salinity Experiment 2000 (WISE 2000): Scientific Analysis Report," ESTEC Contract, Aug. 2001.

[8] J. Miranda, M. Vall-Ilossera, A. Camps, and N. Duffo, "Sea Surface Emissivity at L-band: Swell Effects," *Proc. IGARSS'02*. vol.5, pp. 2623-2625, June 2002.

[9] P. A. Hwang, "Observations of Swell Influence on Ocean Surface Roughness," *J. Geophys. Res.*, vol. 113, no. C12, pp. 2156-2202, Dec 2008.

[10] S. J. Katzberg, O. Torres, and G. Ganoe, "Calibration of Reflected GPS for Tropical Storm Wind Speed Retrievals," *Geophys. Res. Lett.*, vol. 33, no. 8, pp. L18602:1-5, Sep. 2006.

[11] A. G. Voronovich and V. U. Zavorotny, "The Transition From Weak to Strong Diffuse Radar Bistatic Scattering From Rough Ocean Surface," *IEEE Trans. Antennas Propag.*, vol. 65, no. 11, pp. 6029-6034, Nov. 2017.